Danger signals released during cold ischemia storage activate NLRP3 inflammasome in myeloid cells and influence early allograft function in liver transplantation

Fernando Lucas-Ruiz,[a] Sandra V. Mateo,[a,f] Marta Jover-Aguilar,[b,c,f] Felipe Alconchel,[b,c,f] Laura Martínez-Alarcón,[b,c] Carlos de Torre-Minguela,[a] Daniel Vidal-Correoso,[a] Francisco Villalba-López,[a] Víctor López-López,[b,c] Antonio Ríos-Zambudio,[b,c] José A. Pons,[d] Pablo Ramírez,[b,c] Pablo Pelegrín,[a,e,**] and Alberto Baroja-Mazo[a,*]

[a]Molecular Inflammation Group, University Clinical Hospital Virgen de la Arrixaca, Biomedical Research Institute of Murcia (IMIB-Pascual Parrilla), 30120, Murcia, Spain
[b]Transplant Unit, Surgery Service, University Clinical Hospital Virgen de la Arrixaca, Murcia, Spain
[c]Biomedical Research Institute of Murcia IMIB-Pascual Parrilla, Murcia, Spain
[d]Liver Transplantation Unit, Gastroenterology and Hepatology Service, University Clinical Hospital Virgen de la Arrixaca, Biomedical Research Institute of Murcia (IMIB-Pascual Parrilla), 30120, Murcia, Spain
[e]Department of Biochemistry and Molecular Biology B and Immunology, Faculty of Medicine, University of Murcia, 30120, Murcia, Spain

eBioMedicine
2023;87: 104419
Published Online 19 December 2022
https://doi.org/10.1016/j.ebiom.2022.104419

Summary

Background Innate immunity plays a fundamental role in solid organ transplantation. Myeloid cells can sense danger signals or DAMPs released after tissue or cell damage, such as during ischemia processes. This study aimed to identify DAMPs released during cold ischemia storage of human liver and analyze their ability to activate the inflammasome in myeloid cells and the possible implications in terms of short-term outcomes of liver transplantation.

Methods 79 samples of organ preservation solution (OPS) from 79 deceased donors were collected after cold static storage. We used different analytical methods to measure DAMPs in these end-ischemic OPS (eiOPS) samples. We also used eiOPS in the human macrophage THP-1 cell line and primary monocyte cultures to study inflammasome activation.

Findings Different DAMPs were identified in eiOPS, several of which induced both priming and activation of the NLRP3 inflammasome in human myeloid cells. Cold ischemia time and donation after circulatory death negatively influenced the DAMP signature. Moreover, the presence of oligomeric inflammasomes and interleukin-18 in eiOPS correlated with early allograft dysfunction in liver transplant patients.

Interpretation DAMPs released during cold ischemia storage prime and activate the NLRP3 inflammasome in liver macrophages after transplantation, inducing a pro-inflammatory environment that will complicate the outcome of the graft. The use of pharmacological blockers targeting DAMPs or the NLRP3 inflammasome in liver ischemia during static cold storage or through extracorporeal organ support could be a suitable strategy to increase the success of liver transplantation.

Funding Fundación Mutua Madrileña and Instituto de Salud Carlos III, Madrid, Spain.

Keywords: DAMPs; NLRP3; Inflammasome; Cold ischemia; DCD; DBD; Liver transplantation

*Corresponding author. Campus de Ciencias de la Salud, Edificio LAIB, Office 4.21, Ctra. Buenavista s/n, 30120, Murcia, Spain.
**Corresponding author. Campus de Ciencias de la Salud, Edificio LAIB, Office 4.15, Ctra. Buenavista s/n, 30120, Murcia, Spain.
E-mail addresses: alberto.baroja@ffis.es (A. Baroja-Mazo), pablo.pelegrin@imib.es (P. Pelegrín).
[f]Those authors contributed equally to this work.

Research in context

Evidence before this study

"Danger hypothesis" proposed by Polly Matzinger in the early 1990s provides a link between activation of the innate and adaptive immune systems, that could also be applied to solid organ transplantation. Ischemic events affecting donated organs involve the release of danger signals or DAMPs (Danger-associated molecular patterns) from damaged cells to extracellular space. Those DAMPs signal through innate immune cells inducing a proinflammatory environment which can influence the outcome of the graft. NLRP3 inflammasome is one of the principal sensors of DAMPs in innate immune cells, but has also been found in other cells, such as endothelial cells and hepatocytes, and its activation has been related to inflammation, fibrosis, and cell death in the liver. This make the inflammasome one of the most emerging targets, also in liver diseases. It is worth to note that Torreya Capital's Biopharmaceutical Sector Update Market Outlook ranked "Inflammasome Science" as one of the top five biopharma events of 2021.

Added value of this study

Although is widely described that NLRP3 plays a crucial role in ischemia-reperfusion (I/R) injury, most studies have focused on unravelling the mechanisms of the NLRP3 inflammasome activation using warm I/R models, whereas a limited number of works have studied cold storage conditions, principally in animal models. In this regard, we have detected a myriad of DAMPs of different origin in the organ preservation solution (OPS) collected after cold ischemia static storage directly from 79 donated livers in our hospital. These DAMPs present in the end-ischemic OPS (eiOPS) were able to activate the NLRP3 inflammasome in myeloid cells (monocyte/macrophages) of human origin. A higher cold ischemia time and donation after circulatory death (DCD) negatively influenced the DAMP signature. Moreover, the presence of extracellular oligomeric inflammasomes and IL-18 in eiOPS correlated with a poor early allograft function in liver transplant recipients. Therefore, blocking or degradation of different DAMPs, in addition to the direct inhibition of NLRP3 inflammasome, may be an important approach to both reduce the damage evoked by organ storage and improve the outcome of liver grafts. Moreover, the determination of release patterns of DAMPs during ischemia storage could have an added value in terms of better management of marginal organs.

Implications of all the available evidence

Extracorporeal machine perfusion (MP) is emerging into clinical practice to maintain and deliver organs supplied with oxygen and nutrients prior to implantation, and could serve as an excellent platform to test therapeutic drugs during ex vivo liver preservation. Moreover, the more widely implanted postmortem normothermic regional perfusion (NRP) in DCD donors, where femoral vasculature is cannulated to reperfuse and reoxygenate organs while undertaken, might be useful as a first delivery route for drugs designed to inhibit the inflammasome pathway already in the donor.

Introduction

Deceased donor liver transplantation is a routine procedure for the treatment of terminal liver failure and often represents the only chance of a cure.[1] Although donation after brain death (DBD) accounts for the bulk of organ donations, in recent years there has been growing interest in increasing the donor pool.[2] As a result, organ donation after circulatory death (DCD) has been reintroduced and has contributed to increasing the number of donations in many countries.[3] DCD currently accounts for 32% of donations in Spain and was a key factor in reaching the level of 46 donors per million inhabitants in 2017.[4] Likewise, advances in immunosuppressive therapy have had a great impact on the evolution and success of organ transplantation. With the introduction of new immunosuppressive drugs, the incidence of acute rejection has decreased considerably.[5] These drugs inhibit the function of T cells of the adaptive immune system, which are the main effectors of the rejection phenomenon. However, the "danger hypothesis"[6] also provides a link between activation of the innate and adaptive immune systems in transplantation. The innate system is prepared to sense "danger signals", described as danger-associated molecular patterns (DAMPs), and respond to them, generally by creating a proinflammatory environment. DAMPs are formed mainly by self-molecules of the organism that are not usually found extracellularly and appear after tissue damage, such as those produced during ischemia, and can have an impact on the progress of transplantation and even on early rejection events.[7] Among others, heat sock proteins (HSPs), alarmins such as high mobility group box 1 (HMGB1) or the interleukin (IL)-1 family cytokine IL-33,[8] extracellular adenosine triphosphate (ATP), uric acid crystals, free or protein-associated nuclear double-strand DNA (dsDNA), high concentrations of free fatty acids, heparan sulfate proteoglycans, and bile salts stand out as the main DAMPs released after ischemia.[9] Although they take different pathways, all of these DAMPs are able to activate formation of the inflammasome.

The inflammasome is a cytoplasmic multiprotein complex involved in initiating the inflammatory response following a stimulus.[10] This complex is formed by a sensor, which can be NOD-type receptor (NLR) or absent in melanoma 2-like receptor (ALR). The most representative members of these groups are NLRP3 and AIM2, respectively.[11] The first step of canonical inflammasome activation involves the stimulation of Toll-like receptors (TLRs) by pathogen-associated molecular

patterns (PAMPs) or DAMPs and further activation of nuclear factor kappa B (NF-kB). This priming increases transcription of *NLRP3*, *IL1B*, and *IL18*.[12] Subsequently, triggering by DAMPs leads to activation of the NLRP3 inflammasome oligomer and recruitment of the adaptor protein apoptosis-associated speck-like protein (ASC) through a pyrin domain, which, in turn, recruits pro-caspase 1 through CARD–CARD interactions. Inflammasome assembly leads to caspase 1 activation by auto-proteolysis, which will activate the formation of mature IL-1β and IL-18 and lead to cell death by pyroptosis and subsequent release of these cytokines, which then act in an autocrine and paracrine manner on the tissue through IL-1 and IL1-8 receptors, evoking an inflammatory environment.[12] AIM2 is mainly activated by cytosolic dsDNA, while NLRP3 can be activated by a plethora of DAMPs, including several described previously.[13] Inflammasome is mainly found in macrophages, but has also been found in other cells, such as endothelial cells and hepatocytes, and its activation has been related to inflammation, fibrosis, and cell death in the liver.[14]

Here we show how the type of donation, DBD or DCD, or the cold ischemia time (CIT) has an influence in the presence of DAMPs in the organ preservation solution (OPS) collected after cold ischemia and how DAMPs are able to activate the inflammasome in myeloid cells, such as monocytes/macrophages. Moreover, we show the impact of several of these DAMPs in early allograft dysfunction, which could influence graft and patient outcomes.

Methods

Cells and reagents

The human macrophage THP-1 cell line was from the American Type Culture Collection (Cat# TIB-202, RRID: CVCL_0006). HEK-Blue™ TLR4 (Cat# hkb-mtlr4; RRID: CVCL_IM89) and RAW-Blue™ cells (Cat# Raw-sp; RRID: CVCL_X594), Pam3csK4, and anti-TLR2 (Cat# mab2-mtlr2; RRID: AB_1277471) were from InvivoGen (San Diego, USA). *E. coli* lipopolysaccharide (LPS) 055:B5, phorbol 12-myristate 13-acetate (PMA), nigericin, MCC950, cytochalasin D, monodansylcadaverine, N-acetyl-L-cysteine, ATP and A438079 were from Sigma–Aldrich (San Luis, USA). Ac-YVAD-AOM and mitoTEMPO were from Merck-Millipore (Burlington, USA). Proteinase K was from Roche (Basel, Switzerland), DNase I from Qiagen (Hilden, Germany), Uricase from Worthington (Lakewood, USA), anti-HMGB1 (Cat# 651,401; RRID: AB_10945159) from Biolegend (San Diego, USA), and recombinant human IL-18 binding protein (IL-18BP) from GeneScript (Piscataway, USA).

Organ preservation solution collection

In this work, 50 mL of OPS of explanted livers from 79 deceased donors were recovered aseptically after cold ischemia storage and before implantation into the recipient. Donor aorta and donor portal vein were each flushed with 3 L of Celsior® solution (IGL, Lissieu, France) after supraceliac aortic cross-clamping and liver grafts were stored refrigerated at 4 °C in a Celsior® bath. After static cold storage and before implantation, the infrahepatic inferior vena cava was ligated and liver grafts were flushed with 500 mL of 5% human albumin (Grifols, Barcelona, Spain) via the portal vein. At that moment, the first 50 mL of intrahepatic end-ischemic OPS (eiOPS) were retrieved directly from the hepatic veins outflow into the suprahepatic inferior vena cava. eiOPS was stored refrigerated, then centrifuged at 400 ×*g* for 10 min, and supernatants were aliquoted and frozen at –80 °C until use.

Patients

A total of 79 liver transplant patients who received one of the studied donated livers participated in the present study under informed consent; the study was approved by the ethical committee of Hospital Clínico Universitario Virgen de la Arrixaca (2019-6-2-HCUVA) and conforms to the ethical guidelines of the 1975 Declaration of Helsinki. The demographic characteristics of donors and recipients are summarized in Table 1.

Cell culture and monocyte isolation

Cell lines were validated by the corresponding repositories and used before passage 12. The cell lines were regularly tested for mycoplasma contamination using the MycoProbe Mycoplasma Detection Kit (RnD Systems, Cat#CUL001B), and all the experiments were performed using mycoplasma free cells. All cell lines were cultured at 37 °C and 5% CO2 in a humidified incubator.

THP-1 cells were cultured in RPMI medium supplemented with 2 mM of L-glutamine and 10% fetal bovine serum (FBS). Blood from healthy volunteers was collected upon informed consent for monocyte purification. Monocytes were isolated from peripheral blood mononuclear cells (PBMCs) by means of an EasySep Human Monocyte Enrichment Kit without CD16 Depletion (StemCell Technologies, Vancouver, Canada). The purity of monocytes was ≥80%. THP-1 cells were treated with 0.5 μM PMA for 30 min and then primed with 500 ng/mL LPS for 4 h. After that, cells were washed and incubated with eiOPS from liver after cold ischemia. Supernatants were collected after different incubation times and assayed for the presence of IL-1β. Control for canonical NLRP3 inflammasome activation was achieved with nigericin (10 μM) or ATP (3 mM). Isolated monocytes were usually primed with 500 ng/mL LPS and then cultured for different amounts of time with eiOPS. Where indicated, monocytes were directly incubated in eiOPS.

IL-1β determination

IL-1β was measured by an IL-1β Human Instant ELISA kit (Invitrogen, Carlsbad, USA) following the manufacturer's instructions and read in a Synergy Mx plate reader (BioTek, Vermont, USA).

Determination of DAMPs in organ preservation solution

High mobility group box 1 (HMGB1) (Tecan, Männedorf, Switzerland), heat shock protein 70 (HSP70), HSP90 and IL-18BP (Invitrogen), IL-33 (Sigma–Aldrich) and nucleosomes (Merck-Millipore) were determined by ELISA. Uric, bile, and free fatty acids were determined by fluorometric enzymatic assays (Sigma–Aldrich). A Luminex multiplex assay (Invitrogen) was carried out to detect the presence of 9 pro-inflammatory cytokines (IL-6, IL-8, IL-18, IL-1α, IL-10, IL-12p70, IL-17A, IFN-γ and TNFα) and measured in a MagPix System (Luminex, Austin, USA). ATP was quantified by using an ATP Bioluminescent Assay Kit (Sigma-Aldrich),[15] and total free dsDNA was determined by means of a Quant-iT PicoGreen dsDNA Assay Kit (Invitrogen). Caspases activity was measured by monitoring of cleavage of specific fluorescent substrate at 400 nm and 505 nm with a Synergy Mx plate reader (BioTek) for 2 h at 10-min intervals. The presence of endotoxins was measured by a LAL Chromo Endotoxin Quanti Kit (Thermo Fisher Scientific, Waltham, USA) following the manufacturer's instructions. Extracellular oligomeric inflammasome particles was detected as ASC specks[16] on 0.5 mL of eiOPS by flow cytometry using a polyclonal unconjugated rabbit anti-ASC (AL177) antibody (Adipogen Cat# AG-25B-0006, RRID: AB_2490441) at 1:1000 dilution and a secondary Alexa Fluor 647 F (ab') fragment of goat anti-rabbit IgG (H + L) (Invitrogen Cat# A48285, RRID: AB_2896349) at 1:2000 dilution.

Immunofluorescence microscopy

THP-1 cells were seeded in 24-well culture plates (50.000 cells/well) and incubated for 30 min at 37 °C with 0.5 μM PMA, and then cells were primed with 100 ng/mL of LPS overnight in complete DMEM. After priming, the supernatants were removed, washed with ET buffer twice, and incubated with eiOPS for 8 h at

Variables	Donors (n = 79)			p	Recipients (n = 79)
	DBD (n = 49)	DCD (n = 30)			
		SRR (n = 22)	NRP (n = 8)		
Age	60.9 ± 13.6; 65 (22–87)	59.9 ± 13.8; 65 (30–77)	60.4 ± 20.1; 67.5 (26–82)	0.964[a]	57.0 ± 9.6; 59 (24–72)
Sex					
Male	24 (49)	13 (59.1)	5 (62.5)	0.627[b]	44 (64.7)
Female	25 (51)	9 (40.9)	3 (37.5)		24 (35.3)
Body mass index	25.3 ± 4.2; 24.7 (18.4–36.2)	25.1 ± 3.3; 25.3 (16.7–31.6)	28.0 ± 3.4; 28.1 (23.4–32.3)	0.184[a]	26.8 ± 4.2; 26.7 (18.7–36.8)
Cold ischemia (min)	319.5 ± 158.9; 300 (90–960)	366.2 ± 136.5; 333 (180–630)	312 ± 144.6; 283 (150–540)	0.455[a]	
Functional warm ischemia (min)		17.5 ± 7.4; 16 (5–30)	13.4 ± 3.7; 15 (7–18)	0.146[a]	
Diseases					
Alcoholic cirrhosis					37 (46.8)
HCV					8 (10.1)
Arterial thrombosis					6 (7.6)
Primary biliary cirrhosis					5 (6.3)
Cryptogenic liver Cirrhosis					4 (5.1)
NASH					4 (5.1)
HBV					3 (3.8)
Polycystic disease					3 (3.8)
Autoimmune hepatitis					3 (3.8)
Other					6 (7.6)
Re-transplant patients					11 (13.9)
Anastomoses					
With T-tube					25 (31.6)
Without T-tube					54 (68.4)
Exitus at surgery					2 (2.5)
Length of hospital stay (days)					25.21 ± 2.01; 20.5 (1–108)

Continuous variables are expressed as mean ± SD; median (range). Qualitative variables are expressed as frequency (%). DBD, donation after brain death; DCD, donation after circulatory death; NRP, normothermic regional perfusion; SRR, super rapid recovery; HCV, hepatitis C virus; HBV, hepatitis B virus; NASH, non-alcoholic steohepatitis; LT, liver transplantation. [a]One-way ANOVA. [b]Fisher's exact test.

Table 1: **Demographic data of organ donors and recipients included in the study.**

37 °C. As a control, one well was stimulated with 10 μM nigericin for 1 h at 37 °C. After stimulation, the cells were fixed for 15 min at room temperature with 4% formaldehyde in PBS, and then washed 6 times with PBS. Nonspecific binding in cells was blocked with 0.5% bovine serum albumin (Sigma–Aldrich), and cells were permeabilized for 40 min at room temperature with 0.1% Triton-X100 (Sigma–Aldrich) in PBS before incubation for 2 h at room temperature with anti-ASC rabbit polyclonal primary antibody (1:500 dilution; Santa Cruz Biotechnology Cat# Sc-22514-R, RRID: AB_2174874). Cells were washed with PBS and then incubated for 1 h at room temperature with fluorescence-conjugated secondary antibody (Alexa Fluor 488 donkey anti-rabbit IgG, 1:800 dilution; Invitrogen Cat# A-21206, RRID: AB_2535792), then rinsed in PBS and incubated for 10 min with DAPI (1 μg/mL). Cells were washed with PBS 3 times, and images were acquired with a Nikon Eclipse Ti microscope equipped with ×20 S Plan Fluor objective (numerical aperture, 0.45) and a digital Sight DS-QiMc camera (Nikon, Tokyo, Japan) with 387/447 nm and 472/520 nm filter sets (Semrock). Images were achieved with NIS-Elements AR software (Nikon) and analyzed by ImageJ software (US National Institutes of Health).

Liver biopsies procurement

A small piece of biopsy was taken from 6 donated livers (see Table S1 for demographic characteristics) at 2 different times. First, a biopsy was taken before liver procurement, whereas a second biopsy was taken after static cold ischemia storage, just before implantation in the recipient. Both pieces were fixed in PaxGene Tissue Containers (PreAnalytiX GmbH, Feldbachstrasse, Switzerland) and embedded in paraffin.

Liver biopsies immunohistochemistry

An indirect ABC immunohistochemical procedure was performed. Briefly, 3-μm-thick sections of liver samples were analysed by using a specific commercial kit (Vector ImmPress®, Vector Laboratories, Newark, USA) following the manufacturer's recommendations. After deparaffination and rehydration, liver sections underwent a heat-induced demasking antigen procedure (Dako PT-Link, Agilent, Santa Clara, USA) followed by the blocking of endogenous peroxidase and nonspecific background. Liver sections were then incubated overnight with the primary rabbit polyclonal anti-ASC antibody (1:500 dilution; Santa Cruz Biotechnology Cat# Sc-22514-R, RRID: AB_2174874), followed by incubation with the secondary goat anti-rabbit labelled polymer (Vector Laboratories). Immunoreaction was revealed using 3–30-diaminobencicine (DAB) (Vector Laboratories) and counterstained with hematoxylin. The slides were digitalized by using an automatic digital slide scanner (Pannoramic MIDI II, 3D Histech, Budapets, Hungary) with a specific software (Pannoramic Scanner 3.0.2, 3D Histech). Digitalized sections were examined and representative images were also obtained by using a specialized software (Slide Viewer ver. 2.6 (64-bit version), 3D Histech).

Quantitative reverse transcriptase–polymerase chain reaction (qRT-PCR)

Total RNA was extracted from monocytes with an RNAqueous Micro Kit (Invitrogen), or from two 10-μm-thick liver biopsy sections by using RNeasy FFPE kit (Qiagen), followed by reverse transcription. qRT-PCR was performed using SYBR Premix ExTaq (Takara Bio Inc., Kusatsu, Japan). The samples were run in duplicate, and the relative gene expression levels were calculated using the 2-ΔCt method, normalizing to 18SRNA.

Western blot

Detailed methods used for Western blot analysis have been previously described.[17] Immunoblot analysis results were analyzed by densitometry with ImageLab 5.0 software (Bio-Rad, Hercules, USA).

NF-kB reporter experiments

HEK-Blue™ TLR4 and RAW-Blue™ cells were cultured in DMEM high-glucose medium supplemented with 10% FBS, zeocin, and normocin. Cells were plated in a 96-well plate in non-supplemented DMEM and incubated for 16 h with 500 ng/mL of LPS or eiOPS. Supernatants were collected from the wells, and the amount of alkaline phosphatase released into the medium was detected using QUANTI-Blue™ solution (InvivoGen) following the manufacturer's instructions. Briefly, 180 μL of QUANTI-Blue™ solution was added to 20 μL of supernatant in a 96-well plate. Once the mixing was complete, the plate was quickly placed in a microplate reader at 37 °C to measure the optical density at 620–655 nm. A reading was taken every 2 min for 1 h. Finally, the slope of the line was used to estimate the concentration of alkaline phosphatase in the medium.

Model for early allograft function score

The model for early allograft function (MEAF) score was calculated as previously described[18] based on the maximum alanine aminotransferase (ALT) and international normalized ratio (INR) during the first 3 postoperative days and the serum bilirubin on day 3 after transplantation.

Statistical analysis

Statistics were calculated with GraphPad Prism 8.0.2 software (GraphPad Software Inc., San Diego, USA). Data were tested for normal distribution with the

Shapiro–Wilk normality test. The homogeneity of data (homoscedasticity) was analyzed with the F test. A two-tailed unpaired T test for two-group comparison or ANOVA with the Bonferroni post-test for multiple group comparison was used wherever parametrical testing applied (normal distribution and homoscedasticity), and the Mann–Whitney test or the Kruskal–Wallis test with the Dunn post-test was used when the dataset had to be analyzed nonparametrically. Correlation analyses were evaluated by using Spearman's rank correlation. Two-tailed values of $p < 0.05$ were regarded as significant. For all figures, $n \geq 3$ single experiments were performed. eiOPS used for each experiment came from a different pool of donors and each sample was tested in duplicate.

Role of funders

Funding sources provided financial support but had no involvement in study design, collection, analysis and interpretation of data.

Results

Several DAMPs can be detected in the organ preservation solution after liver cold ischemia storage

During cold ischemia, several endogenous molecules are released to the extracellular medium.[9] These molecules can act as DAMPs and activate the immune system. So, we analyzed the presence of different DAMPs in OPS coming from explanted liver and collected after cold ischemia storage. Extracellular ATP, one of the most studied NLRP3 activators, signals through the purinergic P2X7 receptor (P2X7R) in M1 polarized macrophages.[19] However, ATP was undetectable in eiOPS (data not shown). Nevertheless, several DAMPs were detected in eiOPS after cold ischemia (Table 2). Furthermore, other molecules related to inflammasome signaling were detected in the eiOPS, including active caspase-1 and -8, IL-18, and IL-18 binding protein (IL-18BP) (Table 2). However, IL-1β was not detected in the range of pg/mL. Further, IL-6, IL-8, and IL-10 were also detected in eiOPS (Table 2), whereas IL-1α, IL-12p70, IL-17 A, IFN-γ and TNFα were not. Active caspase-3 was also detected in eiOPS, suggesting that during cold ischemia, different types of cell death are induced, including apoptosis and pyroptosis (Table 2). This was further confirmed by the detection of lactate dehydrogenase (LDH) activity in eiOPS (Table 2), indicating that intracellular content was released to the extracellular milieu.

The time during which the liver is in static cold ischemia conditions had an influence in the release of DAMPs; for example, several detected DAMPs had a positive correlation with CIT, including HMGB1, uric acid, HSP70, total free dsDNA, nucleosomes or ASC specks, and IL-18 and its ratio with IL-18BP (Fig. 1a). Also, the type of organ donation affected the concentrations of DAMPs found in eiOPS; in particular, ASC specks, HSP70, IL-33, IL-18, IL-18/IL-18BP ratio, active caspases, and LDH were significantly increased in organs from DCD compared with DBD donors (Fig. 1b), whereas IL-6 was found in higher concentrations in eiOPS from DBD donors (Fig. 1b). Both kinds of donors had similar CIT (Fig. S1). On the contrary, normothermic regional perfusion (NRP) technique showed no differences in DAMPs release with either DCD super-rapid recovery (SRR) donors or with DBD donors (data not shown).

Organ preservation solution from cold ischemic liver activates NLRP3 inflammasome in THP-1 cells and primary monocytes

Different DAMPs are activators of the NLRP3 inflammasome.[20] Therefore, we aimed to find out whether OPS from cold ischemic livers could activate the inflammasome in innate immune cells such as macrophages or monocytes. eiOPS induced the release of IL-1β from LPS-primed THP-1 human macrophages-derived cells after 16 h, but not 4 h of incubation when compared to Celsior® solution as a negative control (Fig. 2a). This release was lower than the induced by the

DAMPs	Concentration
HMGB1 (ng/mL)	119.90 ± 47.28
IL-33 (pg/mL)	97.16 (12.29–639.41)
Nucleosomes (RU/mL)	37 (6–183)
Total free dsDNA (ng/mL)	271.3 (139–1063)
Uric acid (nmol/μL)	0.273 ± 0.122
Bile acid (μM)	55.91 (0–6808)
Free fatty acids (nmol/μL)	0.414 ± 0.188
HSP70 (pg/mL)	51.2 (0–1469)
HSP90 (pg/mL)	81.10 ± 20.76
Free ASC specks (number/mL)	25,762 (1936–303,268)
Endotoxins (EU/mL)	0.077 (0.039–0.242)
Inflammasome related proteins	**Concentration**
IL-18 (pg/mL)	94.51 (0–5998)
IL-18BP (pg/mL)	302.20 (101.1–1175)
IL-6 (pg/mL)	62.94 (0–1059)
IL-8 (pg/mL)	3.24 (0–337)
IL-10 (pg/mL)	0.25 (0–15.39)
Caspase-1 (RU/mL)	37.40 (0–8210)
Caspase-3 (RU/mL)	38.00 (0–5701)
Caspase-8 (RU/mL)	118.80 (0–34,813)
LDH (RU/mL)	2.40 ± 0.55

Variables are expressed as mean ± SD when they followed a normal distribution and as median (range) when they did not. HMGB1, High-mobility group box 1; dsDNA, double strand DNA; HSP, Heat sock protein; ASC, Apoptosis-associated speck-like protein containing a CARD; LPS, Lipopolysaccharide; RU, Relative units; EU, Endotoxin units. RU, Relative units.

Table 2: **Quantification of several DAMPs and different proteins detected in OPS collected after cold ischemia static storage.**

a

	Spearman's rho	HMGB1	dsDNA	Nucleosomes	IL-18	IL-18/IL-18BP ratio	Uric acid	HSP70	ASC specks
CIT	Correlation coeficient	0.283	0.271	0.253	0.321	0.331	0.245	0.426	0.285
	Sig. (2-tailed)	0.011	0.016	0.025	0.004	0.003	0.030	0.0001	0.011
	N	79	79	79	79	79	79	79	79

b

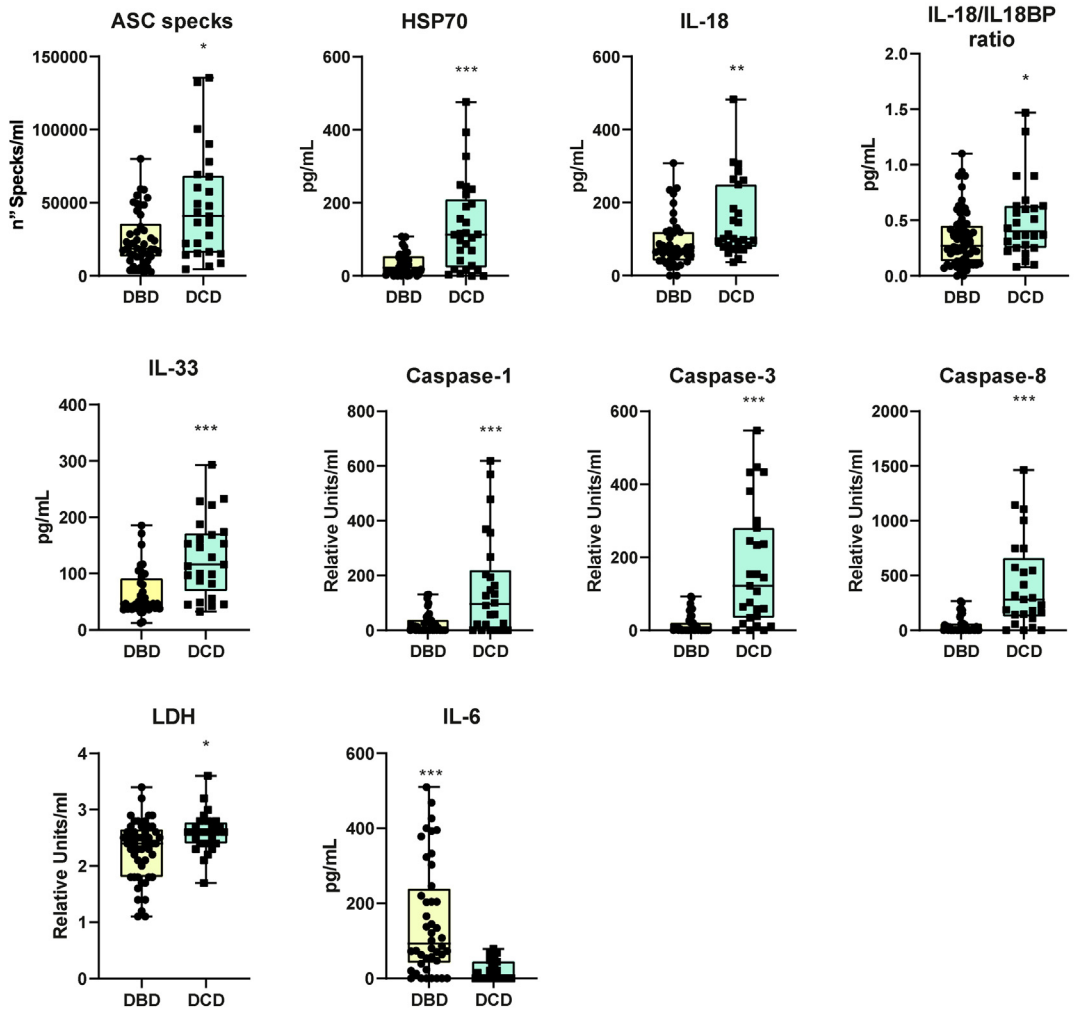

Fig. 1: **DAMPs present in eiOPS are influenced by cold ischemia time and type of donation.** (a) Correlation matrix between CIT and different DAMPs present in eiOPS recovered after cold ischemia storage of liver. (b) Concentration of DAMPs in eiOPS, showing significant differences with regard to type of donation. Each dot represents a single patient; outliers from datasets were identified by the ROUT method, with Q = 1%, and were eliminated from analysis and representation. Results are presented as median, interquartile range, minimum and maximum; each sample was tested in duplicate; $^{*}p \leq 0.05$, $^{**}p \leq 0.01$, $^{***}p \leq 0.001$ [Mann–Whitney test].

potassium ionophore nigericin, a strong NLRP3 activator, but similar to that exerted by ATP (Fig. 2a). The release of IL-1β was inhibited by both the caspase-1 inhibitor Ac-YVAD-AOM and the specific NLRP3 inhibitor MCC950 (Fig. 2b). Moreover, IL-1β release induced by eiOPS was reduced in THP-1 cells deficient in inflammasome component ASC, NLRP3, or caspase-1 (Fig. 2c). On the contrary, when dsDNA present in eiOPS was degraded by DNase I treatment (Fig. S2a), the release of IL-1β remained unaffected (Fig. S2b), suggesting that AIM2 inflammasome activation was not involved. After inflammasome activation, ASC accumulates into a large protein complex termed "speck". Hence, ASC speck development can be used as a simple upstream readout for inflammasome activation.[21] In this regard, the percentage of THP-1 cells containing accumulated ASC or specks also increased after treatment with eiOPS when compared with cells incubated with Celsior® (Fig. 2d).

Likewise, eiOPS was able to activate the inflammasome in human primary monocytes (Fig. 2e). Monocytes primed with LPS for 4 h released IL-1β after incubation for 16 h with eiOPS (Fig. 2e). As observed with THP-1 cells, MCC950 and Ac-YVAD-AOM inhibited eiOPS-mediated IL-1β secretion (Fig. 2e).

We then analyzed the relationship between the different DAMPs present in eiOPS and activation of the NLRP3 inflammasome. Among all analyzed DAMPs, we found that the concentrations of HMGB1, uric acid, HSP70, ASC specks, and IL-18 were positively correlated with the release of IL-1β from THP-1 cells incubated with eiOPS (Fig. 3a). Mechanistically, degradation of proteins (by proteinase K treatment) or uric acid (by uricase treatment) inhibited the activation of NLRP3 mediated by eiOPS (Fig. 3b). On the contrary, inhibition of P2X7R with A438079 had no effect in IL-1β release (Fig. 3b). Beyond specific receptor signaling, clathrin-mediated endocytosis, but not phagocytosis, appeared to be a pathway for inflammasome activation; for example, the presence of monodansylcadaverine (MDC), but not cytochalasin D, was able to inhibit the release of IL-1β from LPS-primed monocytes (Fig. 3c). Likewise, inhibition of reactive oxygen species (ROS), a common signal for NLRP3 activation in response to several triggers,[20] by *N*-acetyl-L-cysteine (NAC), an antioxidant, or mitoTEMPO, a specific scavenger of mitochondrial superoxide, reduced the release of IL-1β induced by eiOPS (Fig. 3d). Furthermore, at the protein level, neutralization of IL-18 and HMGB1 (by incubation with IL-18BP or anti-HMGB1, respectively) inhibited the activation of NLRP3 by eiOPS (Fig. 3e).

Altogether, these data indicate that eiOPS induces the release of IL-1β in innate immune cells through activation of the NLRP3 inflammasome.

Organ preservation solution primes monocytes and induces expression of IL-1β and NLRP3

The first step of NLRP3 inflammasome activation is priming, generally induced by PAMPs and DAMPs, which stimulates TLR receptors and the translocation of NF-κB to the cell nucleus, which in turn increases the transcription of *NLRP3* and the expression of pro-IL-1β.[22] We wanted to find out whether eiOPS was also able to induce NLRP3–inflammasome priming in human monocytes. After monocytes were incubated for 16 h in the presence of eiOPS, there was a significant increase in the expression of *IL6*, *IL1B*, and *NLRP3*, but little increase in *TNFA* (Fig. 4a). At the protein level, variable expression of pro-IL-1β could be detected after incubation with eiOPS from different donors (Fig. 4b). Likewise, each eiOPS sample had a different ability to activate the NF-κB pathway when incubated with the reporter cell line RAW-Blue™ (Fig. S3). We found low levels of endotoxins in the eiOPS (Table 2). However, although LPS concentrations corresponding to those EU/mL (≈0.01 ng/mL) were able to activate HEK-Blue™ TLR4 cells (Fig. S4a), they had no effect on the expression of pro-IL-1β in primary monocytes (Fig. 4c and Fig. S4b). Priming and expression of pro-IL-1β by monocytes after eiOPS activation could be inhibited when TLR2 or clathrin-mediated endocytosis were blocked (Fig. 4d and Fig. S4c). Also, degradation of DNA or proteins by DNase I or proteinase K incubation, respectively, inhibited the priming of these monocytes (Fig. 4d and Fig. S4c).

In response to LPS, human monocytes secrete IL-1β independently of a second signal by means of an alternative inflammasome activation pathway (Fig. 4e and Fig. S4d).[17,23] However, LPS at a low concentration did not activate the inflammasome by the alternative pathway after 16 h of stimulation (Fig. S4d). Likewise, monocytes incubated with eiOPS in the absence of LPS priming had no effect on inflammasome activation (Fig. 4e). However, after 16 h of eiOPS incubation, monocytes were able to release mature IL-1β when activated by nigericin (Fig. 4e). Furthermore, although priming with the synthetic triacylated lipopeptide and TLR2 ligand Pam3CSK4 allowed inflammasome activation mediated by eiOPS incubation, this was significantly lower than that observed after LPS priming (Fig. 4f), even though the expression of pro-IL-1β induced by TLR2 engagement was not significantly different to that induced through TLR4 activation (Fig. 4d and Fig. S4c).

To gain insight about inflammasome activation in the transplanted graft, we took biopsies from 6 consecutive donated livers before (T1) and after (T2) cold ischemia storage. As observed in Fig. 5a, an increased staining for ASC was found in macrophage-like cells within human liver grafts after cold ischemia storage, when analyzed by immunohistochemistry. This is consistent with the increase of the gene expression of ASC in donor tissue (Fig. 5b), similar to the expression of other inflammasome-related genes (*NLRP3*, *CASP1* and *IL1B*) (Fig. 5b). Expression was variable in T1, although relatively higher in DCD livers (Fig. 5b).

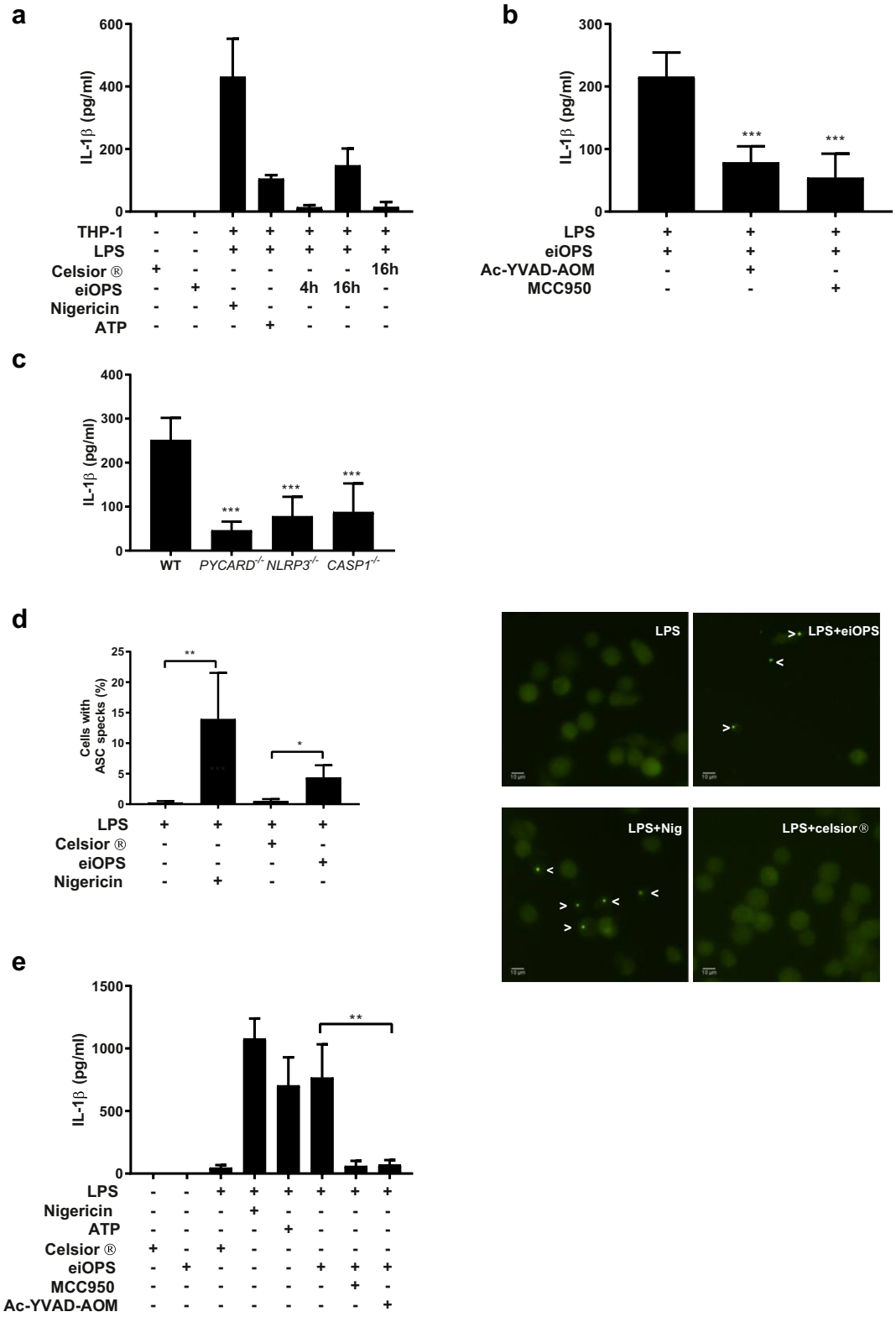

Fig. 2: **eiOPS activates NLRP3 inflammasome in human myeloid cells.** (a) Release of IL-1β by LPS-primed THP-1 cells after incubation with Celsior® or eiOPS for 4 or 16 h. Incubation for 30 min with potassium ionophore nigericin (10 μM) or ATP (3 mM) were used as positive control

DAMPs in eiOPS influence early allograft function in liver transplantation

With the aim to find out whether DAMPs could influence liver transplantation outcomes, we analyzed early allograft dysfunction after liver transplantation by using the MEAF score, which predicts recipient and graft survival.[18] Recipients with DCD grafts had significantly higher scores than those with DBD grafts (Fig. 6a). Moreover, only ASC specks and IL-18 present in eiOPS as well as the IL-18/IL-18BP ratio, which are closely associated with the NLRP3 inflammasome, were found to be positively correlated with the MEAF score (Fig. 6b; Table S2).

Overall, this study suggests that the presence of different DAMPs in eiOPS activates the NLRP3 inflammasome, and this could compromise the outcomes of transplanted livers.

Discussion

Activation of the NLRP3 inflammasome is involved in the progression of liver fibrosis and end-stage cirrhosis, which is among the main etiologies of LT.[24] Moreover, the NLRP3 inflammasome is involved in ischemia–reperfusion injury (IRI)[25] and early inflammation and rejection after LT.[26] We found a plethora of DAMPs released by liver cells during cold static storage that activate the NLRP3 inflammasome in myeloid cells, also in the graft, suggesting that after liver transplantation, NLRP3 could be activated in infiltrated macrophages and resident Kupffer cells, thus inducing a proinflammatory environment in the liver. Nevertheless, beyond myeloid cells, other non-immune liver cells, including hepatocytes and even HSCs, have been reported to activate the NLRP3 inflammasome[27] contributing to liver inflammation and fibrosis,[14,28] hence further analysis of eiOPS-mediated inflammasome activation in those other cells could add valuable information. Our data suggest direct activation of the NLRP3 inflammasome in myeloid cells by several DAMPs released during cold ischemia and disregard the participation of AIM2 inflammasome, as DNA was not involved in the activation, although AIM2 has previously been related to liver inflammation and disease.[29] Although we cannot establish a particular DAMP found in eiOPS as the main trigger of the NLRP3 inflammasome, some of them, such as the alarmin HMGB1, uric acid, HSP70, IL-18, and ASC specks, were shown to have a positive correlation with the release of IL-1β from primed monocytes/macrophages, suggesting that they are the more plausible activators. Nevertheless, and although ATP was not detected in eiOPS, we cannot discard the role of ATP as an important DAMP after tissue damage in transplantation,[30,31] as a fast degradation of extracellular ATP by ecto- and exo-nucleotidases in eiOPS could be happening.[32] Except for uric acid, all of the other mentioned DAMPs are proteins, which is in line with the inhibition exerted by the degradation of proteins in the presence of proteinase K, or, more specifically, by the direct blocking of HMGB1 or IL-18. In this regard, HMGB1, a nuclear protein that participates in nucleosome formation, DNA replication, and DNA repair[33] and was previously characterized in liver IRI,[34] can also act as a DAMP, and even activates the NLRP3 inflammasome in acute glaucoma.[35]

IL-18, a member of the IL-1 family of cytokines, plays an important role in organ transplantation.[36] Our group demonstrated that NLRP3 is activated in the establishment of allograft rejection during mismatched tissue transplantation through IL-18 production.[30] Even more, IL-18 derived from endothelial cells, released during IRI, selectively expands T peripheral helper cells to promote allo-antibody production and chronic antibody-mediated rejection pathologies.[37] Furthermore, our results show that the ratio between the concentrations of IL-18 and IL-18BP released during cold ischemia appears to be correlated with early allograft dysfunction and can be affected by the type of donation or CIT. The pro-inflammatory activity of IL-18 is regulated by the presence of a high-affinity, naturally occurring IL-18BP, that impairs IL-18 from binding to its receptor.[38] Overexpression of IL-18BP suppressed IL-18-induced IFN-γ production, significantly preventing hepatic injury in transplant recipients.[39] With respect to ACS inflammasome oligomers, our group previously showed that upon activation of caspase-1, inflammasome oligomers are released from macrophages, which are then internalized by other macrophages, where they further activate caspase-1 and spread the inflammatory response.[40] In this regard, our results point to endocytosis as an

for NLRP3 activation. Presence of IL-1β in Celsior® and eiOPS before incubation with THP-1 cells was determined as negative control. n = 5. (b) Release of IL-1β by LPS-primed THP-1 cells after incubation with eiOPS for 16 h in the presence of caspase-1 inhibitor Ac-YVAD-AOM (100 μM) or NLRP3 inhibitor MCC950 (10 μM). n = 8. (c) Release of IL-1β by LPS-primed wild-type (WT), *NLRP3*$^{-/-}$, *PYCARD*$^{-/-}$, and *CASP1*$^{-/-}$ THP-1 cells after incubation with eiOPS for 16 h n = 6. (d) Representative microscopy images of ASC specks in THP-1 cells as detected by immunofluorescence, and percentage of THP-1 cells with at least one ASC speck. Quantification of intracellular ASC specks was done from 6 random ×20 images/conditions in at least 3 independent experiments. (e) Release of IL-1β by LPS-primed human primary monocytes after incubation with eiOPS for 16 h in the presence of Ac-YVAD-AOM (100 μM) or MCC950 (10 μM). Incubation with nigericin (10 μM) or ATP (3 mM) after LPS priming were used as canonical NLRP3 activation positive control. n = 5. Representative pictures in (d) are from 4 independent experiments. Results are presented as mean ± SEM; each sample was tested in duplicate; *$p \leq 0.05$, **$p \leq 0.01$, ***$p \leq 0.001$ [one-way ANOVA followed by Bonferroni test (b, c and e) or unpaired Student's t test (d)].

a

	Spearman's rho	HMGB1	Uric acid	HSP70	ASC specks	IL-18
THP1_IL-1²	Correlation coeficient	0.273	0.383	0.259	0.28	0.298
	Sig. (2-tailed)	0.015	0.000	0.021	0.043	0.008
	N	79	79	79	79	79

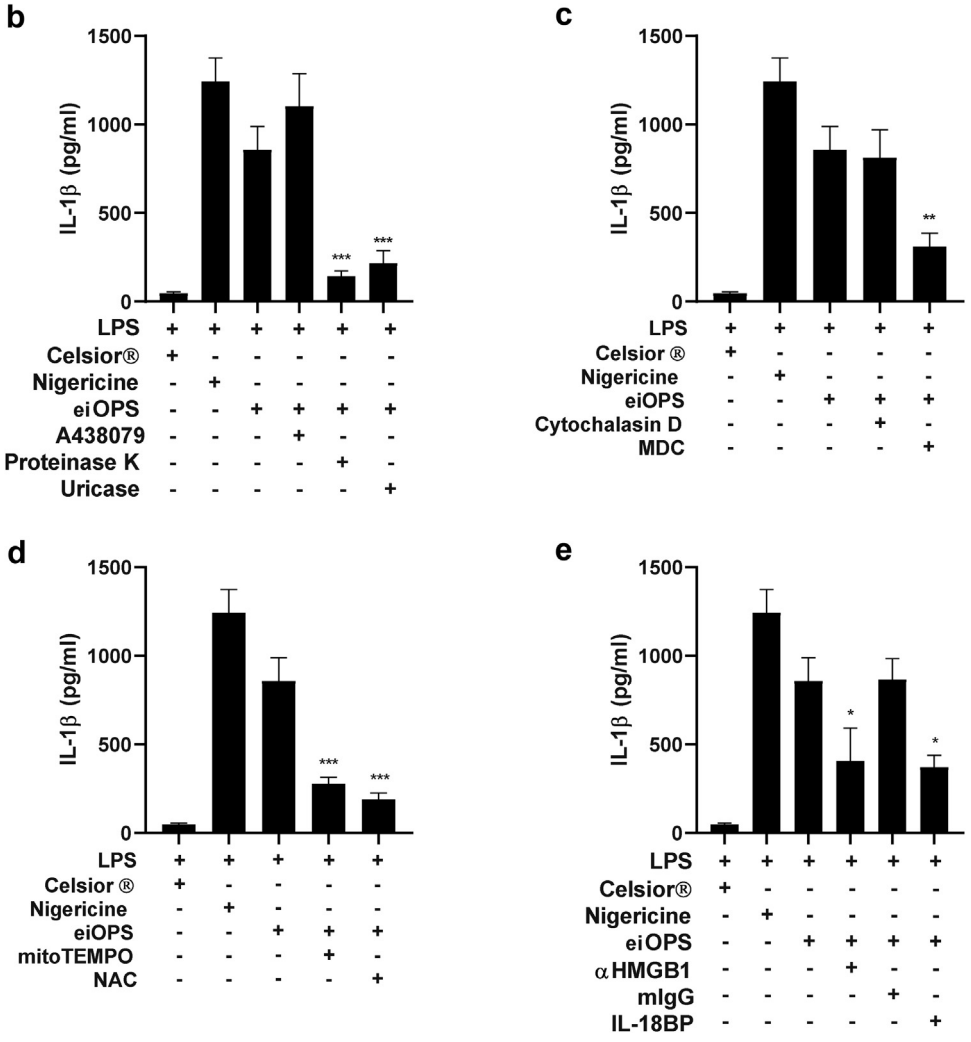

***Fig. 3:* Different DAMPs in eiOPS are able to activate NLRP3 inflammasome in human primary monocytes.** (a) Correlation matrix between concentration of IL-1β released by LPS-primed THP-1 cells after incubation with eiOPS and concentrations of DAMPs present in OPS recovered after cold ischemia storage of liver n = 6. (b–e) Release of IL-1β by LPS-primed human primary monocytes after incubation with eiOPS for 16 h in the presence of specific P2X7R antagonist A438079 (50 μM) (b), phagocytosis inhibitor cytochalasin D (10 μM) or clathrin-mediated endocytosis inhibitor monodansylcadaverine (MDC, 250 μM) (c), specific scavenger of mitochondrial superoxide mitoTEMPO (500 μM) or anti-oxidant *N*-acetyl-L-cysteine (NAC, 10 mM) (d), and IL-18BP (100 ng/mL), anti-HMGB1, or mouse IgG isotype control (100 ng/mL) (e). Alternatively, eiOPS previously incubated with proteinase K (1 mg/mL) or uricase (2 U/mL) was used (b). n = 6. Results are presented as mean ± SEM; each sample was tested in duplicate; $^{*}p \leq 0.05$, $^{**}p \leq 0.01$, $^{***}p \leq 0.001$ [one-way ANOVA followed by Bonferroni test].

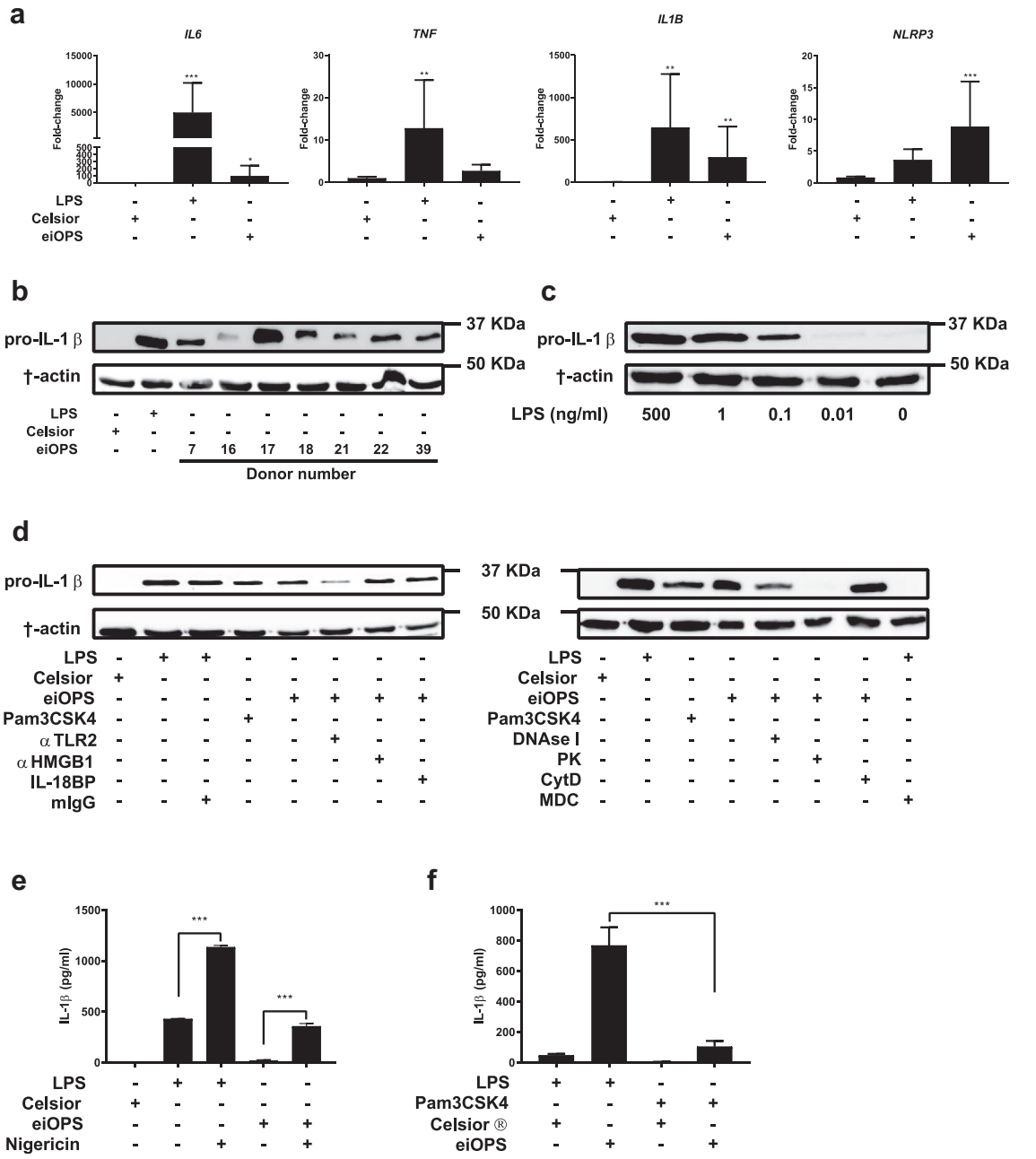

***Fig. 4:* DAMPs in eiOPS prime human primary monocytes.** (a) Fold change of expression of *IL6, TNFA, IL1B*, and *NLRP3* from human primary monocytes treated with LPS (500 ng/mL) or eiOPS for 16 h as detected by RT-qPCR. n = 4. (b–d) Representative cropped Western blots of intracellular pro-IL-1β (Santa Cruz Biotechnologies Cat# sc-7884, RRID: AB_2124476) and β-actin (Santa Cruz Biotechnologies Cat# Sc-47778 HRP, RRID: AB_2714189) from human primary monocytes primed for 16 h with eiOPS from different donors (b); different concentrations of LPS (c); and eiOPS in the presence of cytochalasin D (10 µM), MDC (250 µM), IL-18BP (100 ng/mL), anti-HMGB1 (100 ng/mL), anti-TLR2 (100 ng/mL), and mouse IgG isotype control (100 ng/mL), respectively (d). Alternatively, eiOPS previously incubated with proteinase K (1 mg/mL) or DNase I (100 U/mL) was used, as well as TLR2 activator Pam3csK4 (1 µg/mL) (d). (e) Release of IL-1β from human primary monocytes primed with LPS or eiOPS for 16 h, then activated with nigericin for 2 h. n = 4. (f) Release of IL-1β from human primary monocytes primed for 4 h with LPS or Pam3csK4, then incubated with eiOPS for 16 h. n = 4. Representative images are shown from 3 independent experiments. Results are presented as mean ± SEM; each sample was tested in duplicate; $^{*}p \leq 0.05$, $^{**}p \leq 0.01$, $^{***}p \leq 0.001$ [one-way ANOVA followed by Bonferroni test (a) or unpaired Student's t test (e, f)].

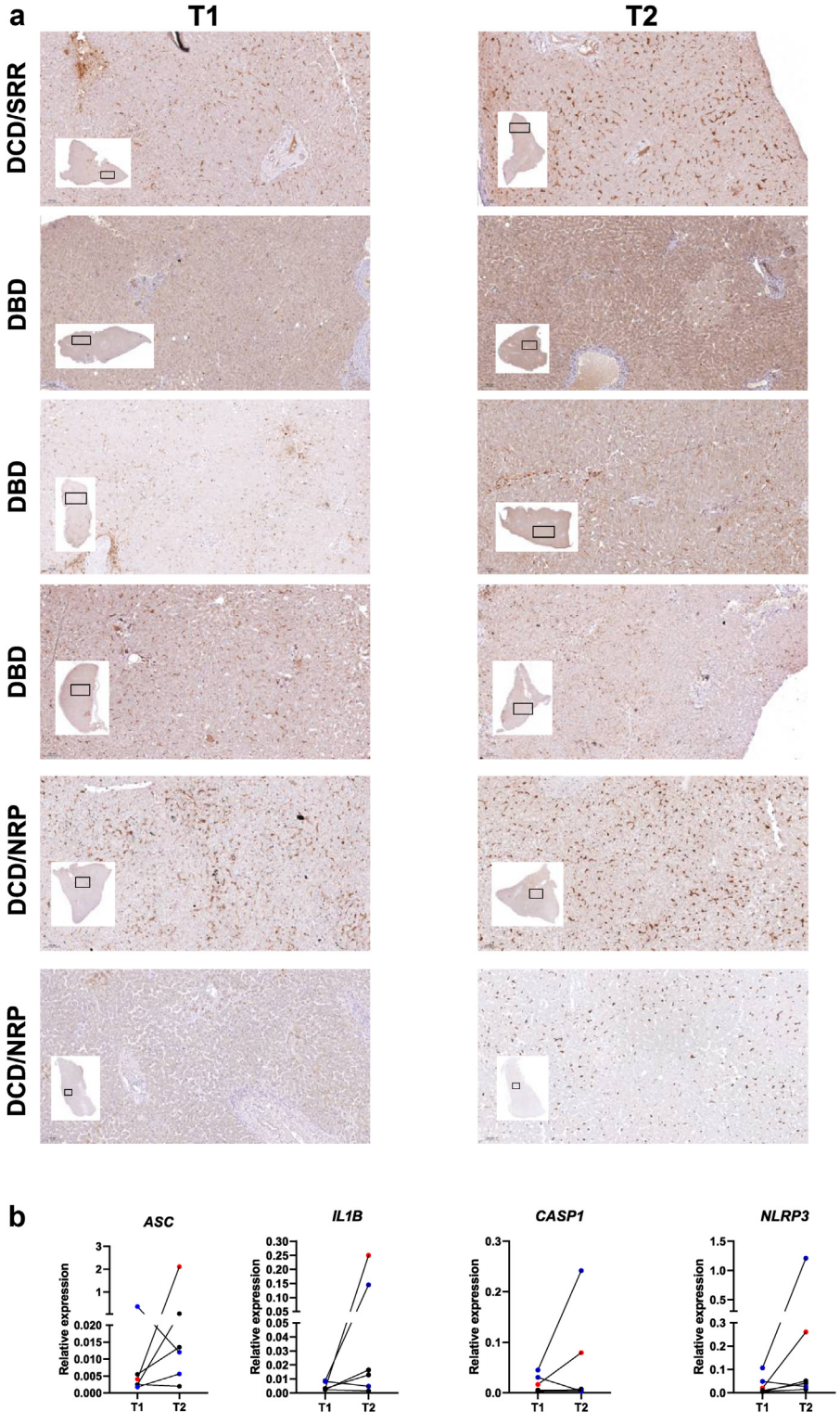

Fig. 5: **NLRP3 inflammasome is increased in the liver graft after cold ischemia storage.** Liver biopsies from donated livers were taken at two different time points: before procurement from the donor (T1), and after static cold storage (before implantation in the recipient) (T2). (a) Representative pictures for each sample as analyzed for immunohistochemistry staining of ASC protein. (b) Relative expression of *ASC*, *NLRP3*, *CASP1* and *IL1B* in tissue biopsies; DBD (black dots), DCD/NRP (blue dots) and DCD/SRR (red dots). n = 6.

a

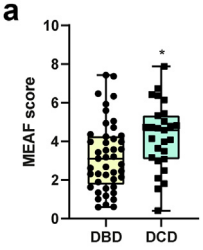

b

	Spearman's rho	ASC specks	IL-18	IL-18/IL-18BP ratio
MEAF score	Correlation coeficient	0.257	0.328	0.296
	Sig. (2-tailed)	0.029	0.005	0.012
	N	72	72	72

***Fig. 6:* DAMPs in eiOPS influence short-term outcome of liver transplantation.** (a) MEAF score for each type of donation. Each dot represents a single patient; results are presented as median, interquartile range, minimum and maximum. Each sample was tested in duplicate; $^{*}p \leq 0.05$ [Mann–Whitney test]. (b) Correlation matrix between MEAF score and ASC specks or IL-18 present in OPS recovered after cold ischemia.

important pathway for the second signal for NLRP3 inflammasome activation mediated by eiOPS. Moreover, activation of NLRP3 in primary human hepatocytes has been shown to lead to pyroptotic cell death and the release of inflammasome oligomers into the extracellular space, leading to hepatic stellate cells (HSCs) activation by particle internalization.[28]

Uric acid, the end product of purine metabolism by the liver,[41] is released from ischemic tissues and dying cells and, when crystalized, is internalized by macrophages, inducing lysosomal membrane damage and activating the NLRP3 inflammasome.[42] Internalization of particulate matter in macrophages results in ROS generation,[43] and increased ROS results in oxidation of thioredoxin (TRX) and its release form TRX-interacting protein (TXNIP), leaving TXNIP free for binding to NLRP3, inducing its activation.[44] This is in line with our results, which show that inhibition of both endocytosis and ROS formation inhibited eiOPS-mediated inflammasome activation. In humans, uric acid crystallization occurs when the level reaches 6.8 mg/dL in plasma.[45] The concentration of uric acid in our eiOPS samples fell into the normal range, although several samples exceeded the limit for crystallization. However, temperature is a factor that appears to play a role in monosodium urate crystal formation through its effects on solubility[46]; for example, a reduction of even 2 °C is sufficient to lower the solubility point of urate in aqueous solution.[47] Nevertheless, soluble uric acid is also able to induce IL-1β release in mouse macrophages, although in humans it is not completely clear.[48] This process is followed by mitochondrial ROS production, ASC speck formation, and caspase-1 activation. Moreover, there is a correlation between soluble uric acid, inflammasome activation, and renal fibrosis.[49]

On the other hand, priming is an indispensable step in NLRP3 inflammasome activation and is usually mediated by PAMPs or DAMPs triggering TLRs.[12] We demonstrate the ability of eiOPS to stimulate TLRs and prime myeloid cells. Scheuermann et al. also showed the presence of HMGB1 and extracellular dsDNA in eiOPS in a rat model of machine preservation of the liver.[50] Our study confirms that these DAMPs are also found in humans and activated TLRs, leading to increased gene expression of *NLRP3* and *IL1B*. Likewise, several DAMPs, such as HSPs, nuclear DNA, HMGB1, and debris produced from the digestion of the extracellular matrix, are associated with tissue injury.[51] Many of them are TLR agonists and NLRP3 inflammasome activators.[52]

One of the better characterized PAMPs is bacterial LPS. Under normal conditions, LPS is undetectable in the systemic circulation, but it has been found at levels up to 1 ng/mL in portal venous blood.[53] Portal venous blood contains the products of digestion, along with antigens and microbial products that originate from bacteria in the small and large intestine. Although we found endotoxins in eiOPS, the composition or concentration was not enough to activate TLR4 in monocytes. Many cells of the innate immune system express the LPS receptor TLR4; however, in the liver, these receptors are continuously exposed to low levels of LPS, resulting in altered responsiveness to potential LPS challenge.[54] Other TLRs, including TLR2 and probably the intracellular DNA receptor TLR9, seem to be the most plausible receptors involved in the priming mediated by eiOPS. TLR2 has been described as being activated by a wide variety of PAMPs, excluding LPS,[55] but also several DAMPs, including HMGB1,[56] histones[57] and HSPs. Histones and DNA are known DAMPs that reside in the nucleus in the form of nucleosomes. Vertebrate free dsDNA has been found to inadequately activate TLR9.[58] However, complexed DNA, either with histones in the form of a nucleosome or with certain DNA-binding proteins, has been demonstrated to induce TLR9-mediated signaling.[58] TLR9 is located in the endosomal compartment, so DNA needs to be endocytosed in order to activate it. We have shown that dsDNA and endocytosis are involved in the eiOPS-induced priming step of myeloid cells. Vertebrate dsDNA is not easily endocytosed, but several proteins that bind DNA facilitate its uptake, including HMGB1-histone complexes.[59] Moreover, endogenous extracellular nucleosomes released after ischemic injury can activate NLRP3 inflammasome through TLR9.[60] Likewise, HMGB1-loaded extracellular vesicles released by LPS-primed macrophages shuttle HMGB1 to target cells by endocytosis, leading to hepatocyte pyroptosis by the activation of NLRP3 inflammasomes.[61] However,

although eiOPS was able to induce both priming and inflammasome assemble in monocytes, both steps were not effective sequentially, as cells were unable to release IL-1β when activated only with eiOPS. eiOPS requires a long time to prime cells, and Celsior™ composition does not favor in vitro cell cultures.[62,63] In addition, the ability of SARS-CoV-2 open reading frame-8b to prime and activate NLRP3 inflammasome was analyzed in vitro after 48 h of activation.[64]

Clearly, our study shows that a larger CIT and type of organ donation have an impact in the signature of DAMPs present in eiOPS, and this could affect early allograft function. Although under continuous improvement, DCD involves warm ischemia time and more complications compared to DBD grafts,[65] consistent with a higher presence of different DAMPs in OPS collected after cold ischemia, as shown above. However, IL-6, a proinflammatory cytokine found in multiple diseases and used for diagnosis,[66] was found to be reduced in DCD livers compared to DBD livers. IL-6 is elevated in the plasma of DBD donors[67] and recipients[68] and is related to complications with liver transplantation. However, there was no difference in IL-6 in heart tissue between DCD and DBD donors as measured by immunohistochemistry in a rat model of ischemia.[69]

Furthermore, the presence of DAMPs can influence the outcome of LT; for example, extracellular inflammasome oligomers and IL-18 presented a positive correlation with a score model (MEAF score) for the continuous grading of early allograft dysfunction. While other recognized scores are binary,[70] MEAF is a continuous score from 0 to 10 that reflects the graft function[18] and has been independently validated,[71] although it cannot be calculated in cases of graft patient death within the first three postoperative days.

Postmortem normothermic regional perfusion (NRP), in which the femoral vasculature is cannulated after death is declared in the hospital to reperfuse and reoxygenate abdominal organs while undertaken for DCD, is being widely implemented as an alternative to super-rapid recovery (SRR).[72] NRP reduces biliary complications, mainly ischemic type lesions, and improves DCD liver graft survival.[73,74] However, we found no differences between NRP and SRR among DAMPs present in eiOPS from DCD livers, although the number of donors in whom NRP was applied was limited in our cohort. Hessheimer et al. recently reported that CIT remains an independent predictor of graft loss among DCD livers with NRP.[75] Extracorporeal normothermic machine perfusion (NMP), thought to preserve organs for transport at body temperature while providing oxygen and nutrients until implantation,[76] could serve as an excellent platform to test therapeutic drugs during ex vivo liver preservation.[77] HMGB1 is a potential therapeutic target[78] by the administration of inhibitors or blocking antibodies.[79] Likewise, IL-18BP has been used safely in clinical trials,[80] and in a hepatic IRI model, its administration inhibited IL-18-induced inflammation, which mitigated hepatic oxidative stress and protected liver structure.[81] Moreover, recombinant uricase is increasingly being used to treat refractory gout.[82] However, the immunogenicity of uricase-based therapies has limited their use,[83] although co-therapy with an immunomodulator might attenuate the appearance of antibodies against the drug, increasing the probability of treatment success.[84] Beyond blocking or degradation of different DAMPs, direct inhibition of NLRP3 inflammasome is gaining strength in the biopharmaceutical sector.[85] Among the various NLRP3 inhibitors, MCC950 is well-studied and has shown relatively better efficacy than other drugs and compounds, although it presents toxicity.[86] Therefore, several clinical trials are being carried out to reduce the complications and toxicity of MCC950 using novel NLRP3 inhibitor compounds.[87]

Although we cannot isolate the effect of DAMPs-mediated inflammation from other cellular processes also affected during tissue injury (i.e. mitochondrial dysfunction, ROS production or ER dysfunction), our study shows that during static cold ischemia storage, the release of different DAMPs with the ability to activate the NLRP3 inflammasome occurs, therefore inhibiting the inflammasome may be an important approach to reduce the damage evoked by organ storage and could improve both the quality of marginal livers and the outcome of liver grafts. The combination of NRP to avoid warm ischemia and NMP to overcome static storage would be the ideal scenario in the future of liver transplantation concerning the control of inflammasome activation. In addition, NRP might be useful as a first delivery route for drugs designed to inhibit the inflammasome pathway already in the donor, along with the use of extracorporeal perfusion as the major delivery system of such drugs.

Contributors

All authors read and approved the final version of the manuscript. A.B-M., P.P. and P.R. participated in the design of the work. A.B-M., P.P., V.L-L., F.A. and P.R. participated in the discussion and review of the manuscript and verified the underlying data. A.B-M., F.L-R., SV.M., C.dT-M., F.V-L. and D.V-C. carried out all the experiments and statistical analysis. A.R-Z., P.R., V.L-L. and F.A. organized the intra-operating room collection of samples. M.J-A. and L.M-A. collected all the clinical data from patients. JA.P. carried out the follow-up of the patients.

Data sharing statement

All datasets and protocols are available from the corresponding authors on reasonable request to corresponding author (alberto.baroja@ffis.es).

Declaration of interests

P.P. is scientific consultant of Glenmak Ltd, FirstThought, Donation and Transplantation Institute and Viva in vitro diagnostics. P.P. is co-inventor on patent application to use NLRP3 inflammasome as biomarker of disease, which have been licensed to Viva in vitro diagnostics S.L, a company co-funded by P.P., A.B.-M. and L.M-A. A.B-M. is co-inventor on provisional patent application of an in vitro method for predicting organ transplant rejection, but declare that the research was

conducted in the absence of any commercial or financial relationships that could be construed as a potential conflict of interest. The rest of authors declare no competing interests.

Acknowledgements

We are particularly grateful for the generous contribution of the patients and the collaboration of Biobank Network of the Region of Murcia, BIOBANC-MUR, registered on the Registro Nacional de Biobancos with registration number B.0000859. BIOBANC-MUR is supported by the "Instituto de Salud Carlos III (proyecto PT20/00109)", by "Instituto Murciano de Investigación Biosanitaria Virgen de la Arrixaca, IMIB" and by "Consejeria de Salud de la Comunidad Autónoma de la Región de Murcia. We would also like to thank Drs. Carlos Manuel Martínez-Cáceres and Jesús de la Peña for their helpful assistance in the immunohistochemical analyses. J.A.P. was funded by Instituto de Salud Carlos III (PI17/00489). A.B-M. was funded by Fundación Mutua Madrileña (AP171362019), Instituto de Salud Carlos III (PI20/00185) and Fundación Séneca (21655/PDC/21). P.P. was funded by grant PID2020-116709RB-I00 funded by MCIN/AEI/10.13039/501100011033, Fundación Séneca (grants 20859/PI/18, 21081/PDC/19 and 0003/COVI/20), Instituto de Salud Carlos III (grant DTS21/00080) and European Research Council (grant ERC-2019-PoC 899636). P.R. was funded by Instituto de Salud Carlos III (PI18/01302). F.L-R. has been co-financed by the European Social Fund (ESF) and the Youth European Initiative (YEI) under the Spanish Seneca Foundation (Spain) 21373/PDGI/20. SV.M. was funded by Instituto de Salud Carlos III (FI21/00073).

Appendix A. Supplementary data

Supplementary data related to this article can be found at https://doi.org/10.1016/j.ebiom.2022.104419.

References

1 Seehofer D, Schoning W, Neuhaus P. Deceased donor liver transplantation. *Chirurgia*. 2013;84(5):391–397.
2 Saidi RF, Hejazii Kenari SK. Challenges of organ shortage for transplantation: solutions and opportunities. *Int J Organ Transplant Med*. 2014;5(3):87–96.
3 Potter KF, Cocchiola B, Quader MA. Donation after circulatory death: opportunities on the horizon. *Curr Opin Anaesthesiol*. 2021;34(2):168–172.
4 Matesanz R, Dominguez-Gil B, Coll E, Mahillo B, Marazuela R. How Spain reached 40 deceased organ donors per million population. *Am J Transplant*. 2017;17(6):1447–1454.
5 Enderby C, Keller CA. An overview of immunosuppression in solid organ transplantation. *Am J Manag Care*. 2015;21(1 Suppl):s12–s23.
6 Matzinger P. Tolerance, danger, and the extended family. *Annu Rev Immunol*. 1994;12:991–1045.
7 Zhai Y, Busuttil RW, Kupiec-Weglinski JW. Liver ischemia and reperfusion injury: new insights into mechanisms of innate-adaptive immune-mediated tissue inflammation. *Am J Transplant*. 2011;11(8):1563–1569.
8 Thierry A, Giraud S, Robin A, et al. The alarmin concept applied to human renal transplantation: evidence for a differential implication of HMGB1 and IL-33. *PLoS One*. 2014;9(2):e88742.
9 Land WG. Emerging role of innate immunity in organ transplantation part II: potential of damage-associated molecular patterns to generate immunostimulatory dendritic cells. *Transplant Rev*. 2012;26(2):73–87.
10 Martinon F, Burns K, Tschopp J. The inflammasome: a molecular platform triggering activation of inflammatory caspases and processing of proIL-beta. *Mol Cell*. 2002;10(2):417–426.
11 Schroder K, Tschopp J. The inflammasomes. *Cell*. 2010;140(6):821–832.
12 de Torre-Minguela C, Mesa Del Castillo P, Pelegrin P. The NLRP3 and pyrin inflammasomes: implications in the pathophysiology of autoinflammatory diseases. *Front Immunol*. 2017;8:43.
13 Broz P, Dixit VM. Inflammasomes: mechanism of assembly, regulation and signalling. *Nat Rev Immunol*. 2016;16(7):407–420.
14 Wree A, Eguchi A, McGeough MD, et al. NLRP3 inflammasome activation results in hepatocyte pyroptosis, liver inflammation, and fibrosis in mice. *Hepatology*. 2014;59(3):898–910.
15 Baroja-Mazo A, Revilla-Nuin B, de Bejar A, et al. Extracellular adenosine reversibly inhibits the activation of human regulatory T cells and negatively influences the achievement of the operational tolerance in liver transplantation. *Am J Transplant*. 2019;19(1):48–61.
16 Rowczenio DM, Gomes SM, Arostegui JI, et al. Late-onset cryopyrin-associated periodic syndromes caused by somatic NLRP3 mosaicism-UK single center experience. *Front Immunol*. 2017;8:1410.
17 Baroja-Mazo A, Compan V, Martin-Sanchez F, Tapia-Abellan A, Couillin I, Pelegrin P. Early endosome autoantigen 1 regulates IL-1 beta release upon caspase-1 activation independently of gasdermin D membrane permeabilization. *Sci Rep*. 2019;9(1):5788.
18 Pareja E, Cortes M, Hervas D, et al. A score model for the continuous grading of early allograft dysfunction severity. *Liver Transpl*. 2015;21(1):38–46.
19 Pelegrin P. P2X7 receptor and the NLRP3 inflammasome: partners in crime. *Biochem Pharmacol*. 2021;187:114385.
20 Weber ANR, Bittner ZA, Shankar S, et al. Recent insights into the regulatory networks of NLRP3 inflammasome activation. *J Cell Sci*. 2020;133(23):jcs248344.
21 Stutz A, Horvath GL, Monks BG, Latz E. ASC speck formation as a readout for inflammasome activation. *Methods Mol Biol*. 2013;1040:91–101.
22 De Miguel C, Pelegrin P, Baroja-Mazo A, Cuevas S. Emerging role of the inflammasome and pyroptosis in hypertension. *Int J Mol Sci*. 2021;22(3):1064.
23 Gaidt MM, Ebert TS, Chauhan D, et al. Human monocytes engage an alternative inflammasome pathway. *Immunity*. 2016;44(4):833–846.
24 Al Mamun A, Akter A, Hossain S, et al. Role of NLRP3 inflammasome in liver disease. *J Dig Dis*. 2020;21(8):430–436.
25 Jimenez-Castro MB, Cornide-Petronio ME, Gracia-Sancho J, Peralta C. Inflammasome-mediated inflammation in liver ischemia-reperfusion injury. *Cells*. 2019;8(10):1131.
26 Hong BJ, Liu H, Wang ZH, et al. Inflammasome activation involved in early inflammation reaction after liver transplantation. *Immunol Lett*. 2017;190:265–271.
27 Wu X, Dong L, Lin X, Li J. Relevance of the NLRP3 inflammasome in the pathogenesis of chronic liver disease. *Front Immunol*. 2017;8:1728.
28 Gaul S, Leszczynska A, Alegre F, et al. Hepatocyte pyroptosis and release of inflammasome particles induce stellate cell activation and liver fibrosis. *J Hepatol*. 2021;74(1):156–167.
29 Lozano-Ruiz B, Gonzalez-Navajas JM. The emerging relevance of AIM2 in liver disease. *Int J Mol Sci*. 2020;21(18):6535.
30 Amores-Iniesta J, Barbera-Cremades M, Martinez CM, et al. Extracellular ATP activates the NLRP3 inflammasome and is an early danger signal of skin allograft rejection. *Cell Rep*. 2017;21(12):3414–3426.
31 Wilhelm K, Ganesan J, Muller T, et al. Graft-versus-host disease is enhanced by extracellular ATP activating P2X7R. *Nat Med*. 2010;16(12):1434–1438.
32 Giuliani AL, Sarti AC, Di Virgilio F. Ectonucleotidases in acute and chronic inflammation. *Front Pharmacol*. 2020;11:619458.
33 Lange SS, Vasquez KM. HMGB1: the jack-of-all-trades protein is a master DNA repair mechanic. *Mol Carcinog*. 2009;48(7):571–580.
34 Han H, Desert R, Das S, et al. Danger signals in liver injury and restoration of homeostasis. *J Hepatol*. 2020;73(4):933–951.
35 Chi W, Chen H, Li F, Zhu Y, Yin W, Zhuo Y. HMGB1 promotes the activation of NLRP3 and caspase-8 inflammasomes via NF-kappaB pathway in acute glaucoma. *J Neuroinflammation*. 2015;12:137.
36 Liu C, Chen J, Liu B, et al. Role of IL-18 in transplant biology. *Eur Cytokine Netw*. 2018;29(2):48–51.
37 Liu L, Fang C, Fu W, et al. Endothelial cell-derived interleukin-18 released during ischemia reperfusion injury selectively expands T peripheral helper cells to promote alloantibody production. *Circulation*. 2020;141(6):464–478.
38 Dinarello CA, Novick D, Kim S, Kaplanski G. Interleukin-18 and IL-18 binding protein. *Front Immunol*. 2013;4:289.
39 Ono S, Obara H, Takayanagi A, et al. Suppressive effects of interleukin-18 on liver function in rat liver allografts. *J Surg Res*. 2012;176(1):293–300.
40 Baroja-Mazo A, Martin-Sanchez F, Gomez AI, et al. The NLRP3 inflammasome is released as a particulate danger signal that amplifies the inflammatory response. *Nat Immunol*. 2014;15(8):738–748.

41 Alvarez-Lario B, Macarron-Vicente J. Uric acid and evolution. *Rheumatology*. 2010;49(11):2010–2015.
42 Hornung V, Bauernfeind F, Halle A, et al. Silica crystals and aluminum salts activate the NALP3 inflammasome through phagosomal destabilization. *Nat Immunol*. 2008;9(8):847–856.
43 Fubini B, Hubbard A. Reactive oxygen species (ROS) and reactive nitrogen species (RNS) generation by silica in inflammation and fibrosis. *Free Radic Biol Med*. 2003;34(12):1507–1516.
44 Zhou R, Tardivel A, Thorens B, Choi I, Tschopp J. Thioredoxin-interacting protein links oxidative stress to inflammasome activation. *Nat Immunol*. 2010;11(2):136–140.
45 Martillo MA, Nazzal L, Crittenden DB. The crystallization of monosodium urate. *Curr Rheumatol Rep*. 2014;16(2):400.
46 Chhana A, Lee G, Dalbeth N. Factors influencing the crystallization of monosodium urate: a systematic literature review. *BMC Musculoskelet Disord*. 2015;16:296.
47 Loeb JN. The influence of temperature on the solubility of monosodium urate. *Arthritis Rheum*. 1972;15(2):189–192.
48 Braga TT, Davanso MR, Mendes D, et al. Sensing soluble uric acid by Naip1-Nlrp3 platform. *Cell Death Dis*. 2021;12(2):158.
49 Braga TT, Forni MF, Correa-Costa M, et al. Soluble uric acid activates the NLRP3 inflammasome. *Sci Rep*. 2017;7:39884.
50 Scheuermann U, Zhu M, Song M, et al. Damage-associated molecular patterns induce inflammatory injury during machine preservation of the liver: potential targets to enhance a promising technology. *Liver Transpl*. 2019;25(4):610–626.
51 Anders HJ, Schaefer L. Beyond tissue injury-damage-associated molecular patterns, toll-like receptors, and inflammasomes also drive regeneration and fibrosis. *J Am Soc Nephrol*. 2014;25(7):1387–1400.
52 Guo LH, Schluesener HJ. The innate immunity of the central nervous system in chronic pain: the role of Toll-like receptors. *Cell Mol Life Sci*. 2007;64(9):1128–1136.
53 Lumsden AB, Henderson JM, Kutner MH. Endotoxin levels measured by a chromogenic assay in portal, hepatic and peripheral venous blood in patients with cirrhosis. *Hepatology*. 1988;8(2):232–236.
54 Crispe IN. The liver as a lymphoid organ. *Annu Rev Immunol*. 2009;27:147–163.
55 Kaisho T, Akira S. Toll-like receptors as adjuvant receptors. *Biochim Biophys Acta*. 2002;1589(1):1–13.
56 Yu M, Wang H, Ding A, et al. HMGB1 signals through toll-like receptor (TLR) 4 and TLR2. *Shock*. 2006;26(2):174–179.
57 Allam R, Scherbaum CR, Darisipudi MN, et al. Histones from dying renal cells aggravate kidney injury via TLR2 and TLR4. *J Am Soc Nephrol*. 2012;23(8):1375–1388.
58 Marsman G, Zeerleder S, Luken BM. Extracellular histones, cell-free DNA, or nucleosomes: differences in immunostimulation. *Cell Death Dis*. 2016;7(12):e2518.
59 Urbonaviciute V, Furnrohr BG, Meister S, et al. Induction of inflammatory and immune responses by HMGB1-nucleosome complexes: implications for the pathogenesis of SLE. *J Exp Med*. 2008;205(13):3007–3018.
60 Huang H, Chen HW, Evankovich J, et al. Histones activate the NLRP3 inflammasome in Kupffer cells during sterile inflammatory liver injury. *J Immunol*. 2013;191(5):2665–2679.
61 Wang G, Jin S, Huang W, et al. LPS-induced macrophage HMGB1-loaded extracellular vesicles trigger hepatocyte pyroptosis by activating the NLRP3 inflammasome. *Cell Death Discov*. 2021;7(1):337.
62 Ferng AS, Schipper D, Connell AM, Marsh KM, Knapp S, Khalpey Z. Novel vs clinical organ preservation solutions: improved cardiac mitochondrial protection. *J Card Surg*. 2017;12(1):7.
63 Janssen H, Janssen PH, Broelsch CE. UW is superior to Celsior and HTK in the protection of human liver endothelial cells against preservation injury. *Liver Transpl*. 2004;10(12):1514–1523.
64 Shi CS, Nabar NR, Huang NN, Kehrl JH. SARS-Coronavirus Open Reading Frame-8b triggers intracellular stress pathways and activates NLRP3 inflammasomes. *Cell Death Discov*. 2019;5:101.
65 Croome KP, Taner CB. The changing landscapes in DCD liver transplantation. *Curr Transplant Rep*. 2020;7:1–11.
66 Unver N, McAllister F. IL-6 family cytokines: key inflammatory mediators as biomarkers and potential therapeutic targets. *Cytokine Growth Factor Rev*. 2018;41:10–17.
67 Piemonti L, Sordi V, Pellegrini S, et al. Circulating CXCL10 and IL-6 in solid organ donors after brain death predict graft outcomes. *Sci Rep*. 2021;11(1):6624.
68 Azarpira N, Nikeghbalian S, Kazemi K, Geramizadeh B, Malekpour Z, Malek-Hosseini SA. Association of increased plasma interleukin-6 and TNF-alpha levels in donors with the complication rates in liver transplant recipients. *Int J Organ Transplant Med*. 2013;4(1):9–14.
69 Li J, Xue C, Ling X, et al. A novel rat model of cardiac donation after circulatory death combined with normothermic ex situ heart perfusion. *Front Cardiovasc Med*. 2021;8:639701.
70 Olthoff KM, Kulik L, Samstein B, et al. Validation of a current definition of early allograft dysfunction in liver transplant recipients and analysis of risk factors. *Liver Transpl*. 2010;16(8):943–949.
71 Rayar M, Levi Sandri GB, Cusumano C, et al. A score model for the continuous grading of early allograft dysfunction severity. *Liver Transpl*. 2016;22(6):859–860.
72 Jochmans I, Hessheimer AJ, Neyrinck AP, et al. Consensus statement on normothermic regional perfusion in donation after circulatory death: report from the European Society for Organ Transplantation's Transplant Learning Journey. *Transpl Int*. 2021;34(11):2019–2030.
73 Hessheimer AJ, Coll E, Torres F, et al. Normothermic regional perfusion vs. super-rapid recovery in controlled donation after circulatory death liver transplantation. *J Hepatol*. 2019;70(4):658–665.
74 Watson CJE, Hunt F, Messer S, et al. In situ normothermic perfusion of livers in controlled circulatory death donation may prevent ischemic cholangiopathy and improve graft survival. *Am J Transplant*. 2019;19(6):1745–1758.
75 Hessheimer AJ, de la Rosa G, Gastaca M, et al. Abdominal normothermic regional perfusion in controlled donation after circulatory determination of death liver transplantation: outcomes and risk factors for graft loss. *Am J Transplant*. 2021;22:1169.
76 van Beekum CJ, Vilz TO, Glowka TR, von Websky MW, Kalff JC, Manekeller S. Normothermic machine perfusion (NMP) of the liver - current status and future perspectives. *Ann Transplant*. 2021;26:e931664.
77 Dengu F, Abbas SH, Ebeling G, Nasralla D. Normothermic machine perfusion (NMP) of the liver as a platform for therapeutic interventions during ex-vivo liver preservation: a review. *J Clin Med*. 2020;9(4):1046.
78 Wang H, Li W, Goldstein R, Tracey KJ, Sama AE. HMGB1 as a potential therapeutic target. *Novartis Found Symp*. 2007;280:73–85. discussion -91, 160-4.
79 Nishibori M, Mori S, Takahashi HK. Anti-HMGB1 monoclonal antibody therapy for a wide range of CNS and PNS diseases. *J Pharm Sci*. 2019;140(1):94–101.
80 Gabay C, Fautrel B, Rech J, et al. Open-label, multicentre, dose-escalating phase II clinical trial on the safety and efficacy of tadekinig alfa (IL-18BP) in adult-onset Still's disease. *Ann Rheum Dis*. 2018;77(6):840–847.
81 Ozsoy M, Gonul Y, Bal A, et al. Effect of IL-18 binding protein on hepatic ischemia-reperfusion injury induced by infrarenal aortic occlusion. *Ann Surg Treat Res*. 2015;88(2):92–99.
82 Weaver JS, Vina ER, Munk PL, Klauser AS, Elifritz JM, Taljanovic MS. Gouty arthropathy: review of clinical manifestations and treatment, with emphasis on imaging. *J Clin Med*. 2021;11(1):166.
83 Schlesinger N, Padnick-Silver L, LaMoreaux B. Enhancing the response rate to recombinant uricases in patients with gout. *BioDrugs*. 2022;36:95–103.
84 Sands E, Kivitz A, DeHaan W, Leung SS, Johnston L, Kishimoto TK. Tolerogenic nanoparticles mitigate the formation of anti-drug antibodies against pegylated uricase in patients with hyperuricemia. *Nat Commun*. 2022;13(1):272.
85 Moeller-Gorman R. Pharma looks to inflammasome inhibitors as all-around therapies. *Scientist*. 2021. serial on the Internet.
86 Bakhshi S, Shamsi S. MCC950 in the treatment of NLRP3-mediated inflammatory diseases: latest evidence and therapeutic outcomes. *Int Immunopharmacol*. 2022;106:108595.
87 Corcoran SE, Halai R, Cooper MA. Pharmacological inhibition of the nod-like receptor family pyrin domain containing 3 inflammasome with MCC950. *Pharmacol Rev*. 2021;73(3):968–1000.